JOURNAL OF COMPUTATIONAL PHYSICS **135,** 141–148 (1997)
ARTICLE NO. CP975723

Clouds-in-Clouds, Clouds-in-Cells Physics for Many-Body Plasma Simulation[1]

Charles K. Birdsall[2] and Dieter Fuss

Lawrence Radiation Laboratory, University of California, Livermore, California 94550

Received August 22, 1968

A clouds-interacting-with-clouds, clouds-in-cells method (ClC) is presented for many-body nonlinear plasma problems. Density and force are obtained by assuming that the particles have finite size, are tenuous, and may pass through one another; the particles are thus called clouds. They obey a Coulomb force ($\sim 1/r$ or $1/r^3$) when separated and a linear force ($\sim r$) when overlapping, allowing simple harmonic oscillations at small separation. CIC is contrasted with the zero-size particle and nearest-grid-point approach, ZSP–NGP. CIC appears to have substantially less unwanted noise than ZSP–NGP and should be more useful in simulating dense plasmas. Initial runs have been encouraging. The methods may find use in other many-body simulations, such as with stars, or with particles in phase space.

INTRODUCTION

A clouds-interacting-with-clouds, clouds-in-cells (CIC) method is being used with some advantage over a zero-size-particle approach, especially with regard to reducing errors in the calculation of density and force. A major application is to many-body, nonlinear effects in fusion plasmas, and initial results with a two-dimensional code, SQRPLA, have been encouraging [1].

1. PROBLEM STATEMENT

The problem is to obtain the motion of ions and electrons in their own and applied fields. The electrostatic potential ϕ is obtained from the electric charge density ρ by solving Poisson's equation,

$$\nabla^2\phi = -\frac{\rho}{\varepsilon_0}$$

using a 48×48 grid, with ϕ obtained at the grid points. We use a 9-point difference equation for Poisson's equation (suggested by M. Greenberg) as given in Appendix A. The motion of the individual charged particles is obtained by integrating the Newton–Lorentz equation,

$$m\frac{\partial \mathbf{v}}{\partial t} = q(\mathbf{E} + \mathbf{v} \times \mathbf{B}).$$

The electric field $\mathbf{E}$ is $-\nabla\phi$. The magnetic field $\mathbf{B}$ is the applied field, given analytically. This integration uses the orbit fitting scheme given by Hockney [2].

The special problem addressed here is how to convert charge positions into charge density, and then how to obtain a consistent force on the particles.

2. ZERO-SIZE-PARTICLE DENSITY AND FORCE

In the zero-size-particle and nearest-grid-point method (ZSP–NGP), charge density is obtained by putting the charge and mass of a particle at the nearest grid point; the force is evaluated as if the particle were at the grid point. These choices produce zero self-force, as desired. The resultant force law (in two dimensions) between two like particles approximates a $1/r$ Coulomb law, in staircase fashion, down to separation of one cell where the force vanishes; the ZSP–NGP force law is shown in Fig. 1, from Hockney [2]. The stepped law is inaccurate and the zero force region wipes out plasma oscillations for separations between ions and electrons of less than one cell even for long wavelengths. Hockney [5] proposes that these difficulties can be reduced by using a very large number of particles in a Debye circle, $N_D \equiv n\pi\lambda_D^2 \gg 1$; n is the number density of ions or electrons and λ_D is the Debye length, $v_{\text{thermal}}/\omega_p$, where ω_p is the plasma frequency (simple harmonic oscillation frequency for small perturbations from equilibrium). However, with limited computer memories and times, the number cannot be increased indefinitely, limiting ZSP–NGP to low plasma densities.

Reprinted from Volume 3, Number 4, April 1969, pp. 494–511.

[1] This work was performed under the auspices of the U.S. Atomic Energy Commission.

[2] Permanent address: Electrical Engineering and Computer Sciences Department, University of California, Berkeley, CA. This author was supported in part by A.E.C. Contract AT-(11-1)-34Proj. 128).

0021-9991/97 $25.00

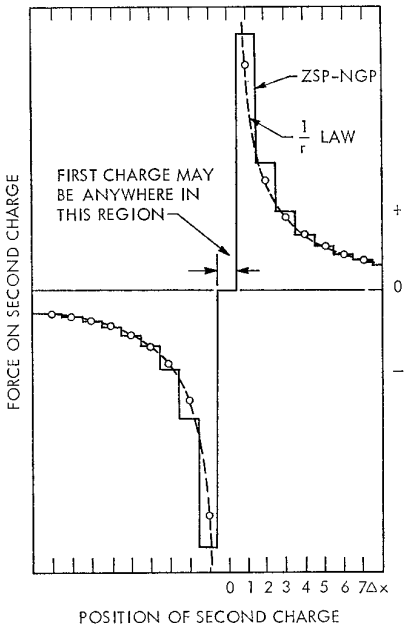

FIG. 1. Zero-size-particle, nearest-grid-point force between two positive particles. Force is zero in region $-\Delta x/2 < x < \Delta x/2$. Adapted from Fig. 10 of Hockney [2].

3. CIC DENSITY

In the CIC method the particle coordinates (x, y) are taken to be at the center-of-mass-and-charge of charged clouds of finite extent. The clouds are tenuous and may pass through one another. The approach was first suggested to us by J. A. Byers; a similar interpretation was mentioned by Hockney [2]. The charge density to be assigned to points in a spatial grid is obtained by sharing the charges at several points. For example, using a cloud the same size as a grid cell, Δx by Δy, as shown in Fig. 2, the charge in the area shaded (═) is assigned to grid point (i, j), that shaded (||||) to $(i + 1, j)$, that shaded (▨) to $(i + j, j + 1)$, and that shaded (////) to $(i, j + 1)$. For a large number of clouds, the charge density at (i, j) is obtained by summing over the clouds as

$$\rho(i,j) = \sum_{\text{clouds}} a_{ij}\rho_c(x,y),$$

where $\rho_c(x, y)$ is the density of the cloud at x, y and a_{ij} is the area of the cloud appearing in the cell centered at i, j divided by the area of the cell; see Appendix B.

The cloud size need not be that of a cell. As the cloud size is increased from zero, the force law begins to be smoothed out and the zero force region shrinks; the staircasing and zero-force region are absent for cloud size equal to cell size. The density appearing at i, j for a cloud moving along x is shown in Fig. 3 for square clouds of side $H = 0$ through $H = 2\Delta x$. As the cloud size is increased beyond cell size, resolution decreases because the cloud density is held constant over a distance larger than the shortest resolvable wavelength. Of course, the density could vary within a cloud, which would be resolvable only if the cloud is larger than a cell or, as H. Berk suggests, the cloud size might vary during the problem. The method centers around reducing the potential energy of the particles as we go from a laboratory system of, say, 10^{15} particles to a computer experiment with, say, 10^4 particles; the greatest improvement comes with the greatest overlapping of clouds.

The potential energy is presently calculated by summing $\rho\phi$. The ρ's are the charge densities assigned to the grid points and the ϕ's are the potentials at the grid points. With this method, as an isolated cloud moves through the mesh, the potential energy is not constant, but largest for the cloud at a grid point and least in between. With many charges, these variations are small, but still undesirable.

4. CIC FORCE

The CIC method uses the electric force on a cloud as that averaged over the cloud, as given by

$$\mathbf{E}(x,y)_{\text{effective}} = \sum_{\text{cloud}} a_{ij}\mathbf{E}_p.$$

The a_{ij} are the fractional areas as before; the $\mathbf{E}_p$ are the fields at the grid points where the parts of the cloud are assigned. For example, for that part of the cloud placed at the point $i + 1, j + 1$, the x-field is given by

$$-(\phi(i+2, j+1) - \phi(i, j+1))/2\Delta x.$$

It is obvious that in an infinite net (walls well removed) the partial cloud produces no force on itself; A. B. Langdon has shown us that partial clouds, taken pairwise, produce equal and opposite forces, explosive in nature, producing no net self (translational) force since the cloud has an

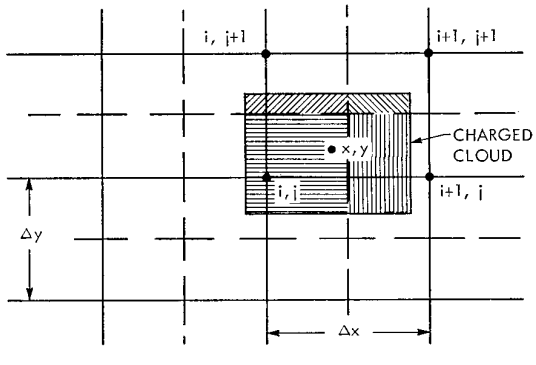

FIG. 2. Cloud located in a grid, with shading showing assignment of density to grid points for CIC method.

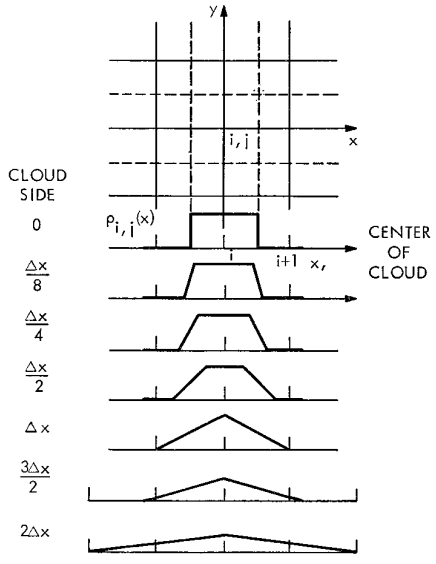

FIG. 3. Sketch of charge density assigned to (i, j) as particle moves past this grid point. The size of the cloud in the x direction (cloud side) varies from 0 to $2\Delta x$.

implicit binding force. Thus, the CIC choices of charge and force sharing also produce no self force. The CIC force law is sketched in Fig. 4.

One peculiarity of the square clouds in the square net is that the force between two charged particles is not wholly a central force. Because of the four-pole nature of the cloud there is a small azimuthal force which varies periodically aximuthally (as does the central force). This causes two overlapping clouds which are oscillating in simple harmonic (ω_p) motion to have an added azimuthal precession, first seen by D. Wong in our 3D program, CUBic PLAsma. C. Leith points out that this will tend to produce some angular squeezing, in our model, about a grid rotated $\pi/4$ from the x, y grid. Remedies are to use larger clouds (more poles, more rapid decay of multipolar terms) or, more radically, a ''rounder'' grid (e.g., hexagonal); use of circular clouds with the square grid does not appear too promising, as the grid effect remains.

CIC is essentially a sharing rule for finding density and force, and proceeds just as in ZSP–NGP once the sharing is found.

5. DENSITY CONTOURS

The step from ZSP–NGP to CIC goes in the direction of particle to fluid mechanics. The ZSP–NGP density assignment is that the particle is either in or out of a given region. A way of illustrating this is by a contour plot of density as a particle with coordinates x, y moves in the region $i \pm 1, j \pm 1$, shown in Fig. 5. If the ZSP–NGP particle is within half a cell from the point i, j then the density is 1, otherwise, 0. In contrast, the density contours for CIC, Fig. 6, show a smooth transition from 0 to 1 over the whole region. For both models, in the region shown $(i \pm 1, j \pm 1)$ the average density at point (i, j) is 1/4, assuming that the particle has uniform probability of being in this region. For CIC, the figure of 1/4 can also be interpreted as meaning that a particle is equally shared with four points, on the average.

6. SPATIAL SPECTRA

Let us look at the spectra of charge density to see what errors are produced in the electric field because of the sampling in space.

As a charge moves from cell i to cell $i + 1$, the densities assigned in ZSP–NGP to the grid points in the center of these cells vary as shown in Fig. 7a; as the particle position x passes halfway between i and $i + 1$, the density at i jumps to zero and the density at $i + 1$ to full value. Hence, point i senses a thick particle which is Δx on a side. For a rough measure of the apparent wavelengths produced, or spatial spectrum, we take the Fourier transform of this apparent density, which is simply $\sin(k\Delta x/2)/k\Delta x/2)$, as sketched in Fig. 7b. Note that the grid does not respond correctly to information for $k\Delta x > \pi$; such information is falsely translated to longer wavelengths (aliased).

In CIC, the corresponding behavior is shown in Fig. 8, the Fourier transform being the square of that above. By spreading out the charge, the spectrum is narrowed so that the amount of information that can be aliased is greatly reduced. One may choose to use larger clouds in order to reduce the spatial spectrum; or, if in the process of analysis the Fourier spectrum of the density is available, the spectrum can simply be narrowed to make small clouds appear larger (suggested by A. B. Langdon). If we take the information aliased to be related to the energy, then we should

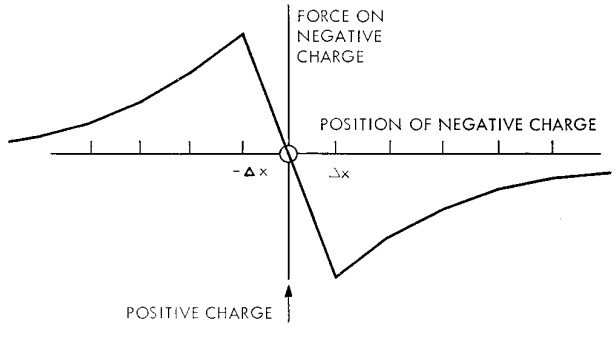

FIG. 4. Force between a fixed positive charged cloud at a grid point and a negative cloud with the same y coordinate. The force approximates by straight line sections the Coulomb $1/r$ force down to small separation where the law becomes linear; the clouds have simple harmonic plasma oscillation for small separation. For other cloud locations in the grid, the details differ slightly.

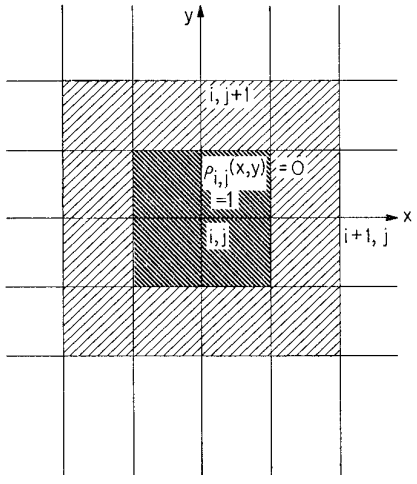

FIG. 5. ZSP–NGP density at (i, j) for a particle at x, y; $(i-1)\Delta x < x < (i+1)\Delta x$, $(j-1)\Delta y < y < (j+1)\Delta y$.

look at the square of the spectrum, in Fig. 8b, the solid curve is $\rho_i^2(k)$ for ZSP–NGP and the dashed curve is $\rho_i^2(k)$ for CIC. If we let the information aliased be proportional to the area under each curve for $k\Delta x > \pi$, then ZSP–NGP has an area almost an order of magnitude greater than CIC in this region.

7. TIMING ERRORS

The errors in time may be thought to occur because the particle arrives and leaves early or late at a given cell position because of the discrete sampling in time. These errors are aggravated by the size of the particle (as contrasted with a smooth fluid). This effect is shown in Fig. 9 for ZSP–NGP. With an average velocity $\bar{v}$, the average time used in crossing a cell of side h is called $T(\bar{v}T = h)$, the transit time. As time advances in steps Δt, a charge may depart late by δt from one cell, hence arriving late by the same amount in the next cell, $\delta t < \Delta t$. If there are many particles in a cell on the average, there will be about as many arriving late as there are leaving late so that these errors will tend to cancel and produce the correct value of total charge in a given cell. The corresponding error in the vector direction of **E**, an error which occurs in two and three dimensions, may not be compensated this way. Unfortunately, we may not always have many particles per cell; indeed, we are more likely to average less than ten, with incomplete compensation between entering and leaving particles. For purposes of estimating the size of the error, we will use only one particle.

The early–late arrival depends on the integration scheme for the equation of motion. We use the method as given by Hockney [2], with time steps shown in Fig. 10. The charge positions give the charge densities and the electric field; from **E**, the velocity **v** is advanced, and from the new value of **v**, the particles are advanced, each of the two steps being time-centered. Thus, given the position, the charge density is assumed constant for Δt about time t.

For ZSP–NGP, the magnitude of charge will be too small by q for δt and then T later, too large by q for δt. The range of δt is $0 < \delta t < \Delta t$ and the average value would appear to be $\bar{\delta} \cong \Delta t/2$. One viewpoint is to say that the measured value of $\rho_i(t)$ is the sum of the "true" value $(\Delta t \to 0)$ plus an error term. For ZSP–NGP, the magnitude of the error term is q and its frequency spectrum will be quite broad, extending well beyond the time resolution available. This extension is a measure of information lost or noise added to the computation.

For CIC, a similar diagram can be made (Fig. 11). The peak error is less and the frequency spectrum of the error is narrower, as the error is nearly periodic with period Δt; hence there is less lost information or noise. One other point is that the peak value of the charge for CIC (b) will in general be less than that for ZSP–NGP (a), (the whole charge) because the cloud on the average is shared with four grid points. Hence, using

$$c \cong \frac{b\Delta t/2}{T} \quad \text{and} \quad b \cong a/4$$

we estimate

$$c \cong \left(\frac{\Delta t}{8T}\right) a,$$

which is a decrease in the direct error of at least an order of magnitude, possibly much more in the mean square error.

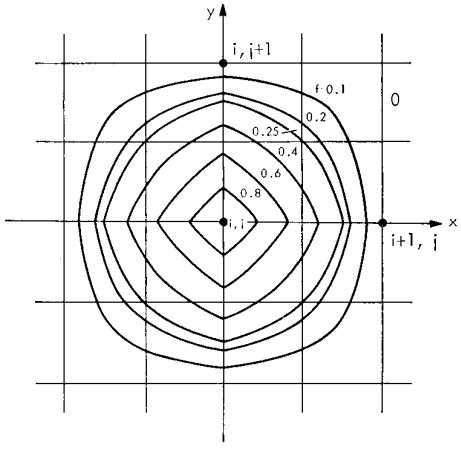

FIG. 6. CIC density contours at (i, j) for a cloud at x, y; $(i-1)\Delta x < x < (i+1)\Delta x$, $(j-1)\Delta y < y < (j+1)\Delta y$. Cloud = cell size.

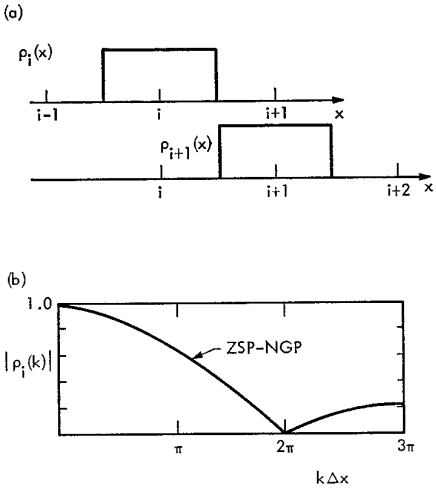

FIG. 7. ZSP–NGP density spatial assignment and Fourier spatial spectrum.

8. SHOT NOISE, FLUCTUATIONS

A classical approach can be used to estimate a collision rate or diffusion due to computational discreteness in time and space. Let us again make rough estimates. For a gas of independent and noninteracting particles, the dispersion about the mean value of the number in some volume is

$$\frac{\overline{\delta n^2}}{\overline{n}^2} = \frac{1}{\overline{n}}.$$

If we choose the volume in question to be the least volume discernible, roughly one cell, then $\overline{n}$ will generally be on the order of 1 to 10 and the dispersion will be large indeed. H. Berk suggests that the volume in question should have sides on the order of $(1/k)$, where k is the largest wavenumber of interest.

A special volume for plasmas is that bounded by λ_D on a side. For smaller volumes there can be appreciable charge separation with correspondingly large electric fields; for larger volumes, the charge separation and E fields will be smaller. Hence, one might expect the dispersion to be about $1/\overline{n}$ for volumes up to $\overline{n} = N_D$ but to be much smaller than $1/\overline{n}$ (or $1/N_D$) for larger volumes.

If we take the dispersion to be the fluctuations in charge density due to discreteness and let these fluctuations produce a fictitious electric field, $\overline{E_f^2}$, then we obtain an effective collision frequency which is proportional to $\overline{E_f^2} \sim \overline{\delta n^2}$. This collision frequency would overestimate the effect of fluctuations because the particles interact dynamically in such a way as to smooth out fluctuations rather completely at low frequencies and at distances greater than λ_D. Thus, even for a laboratory plasma we might write something like

$$\frac{\overline{\delta n^2}}{\overline{n}^2} = R^2\left(\frac{1}{n}\right).$$

R^2 is the dynamical fluctuation (or shot noise) reduction factor, generally expected to be less than unity and dependent on frequency, wavelength, and the volume in question, i.e., $R^2 = R^2(\omega, k, \overline{n}/N_D)$. From the physics of laboratory plasmas, one should be able to obtain the ω, k dependence of R^2; such answers may be quite complex and obtained after considerable effort, as exemplified by similar calculations of diode noise [4]. Answers for simulation noise may be expected to be somewhat more difficult to extract. Hockney [2, 5] has offered some values which may be applicable to ZSP–NGP but which may overestimate the noise in CIC.

Some answers are available. A $1/\overline{n}$ dependence has been observed by Barnes and Dunn [3] for shot noise using a one-dimensional electron model, about λ_D in length, with zero-size particles; from their work we find that $R^2 \cong 3 \times 10^{-4}$ is implied, showing considerable interaction. The arguments given earlier imply that short-wavelength, high-frequency fluctuations should be reduced as H is increased from zero; the reduction in fluctuations, $\langle E^2(k)\rangle$, at large k has recently been shown in theory and experiment by Dawson, Hsi, and Shanny [6] for Gaussian density slabs and by McKee [7] for uniform density slabs. The total fluctuation level is also reduced by the use of clouds, with appreciable reduction coming as the cloud is made larger than a Debye volume, i.e., $H > \lambda_D$. For such large clouds, the shielding length changes from λ_D to H, as originally suggested to us by J. M. Dawson and shown explicitly recently by H. Okuda for a special cloud [7].

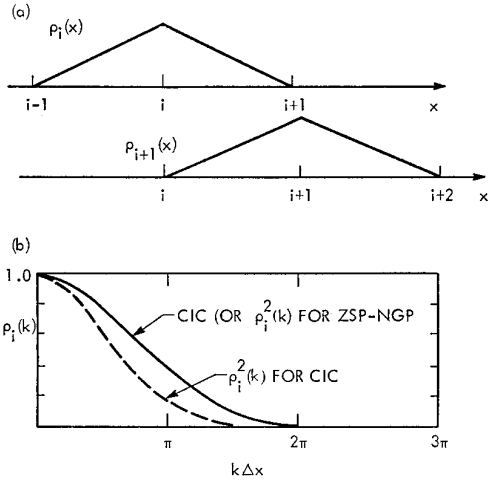

FIG. 8. CIC density spatial assignment and spatial spectrum.

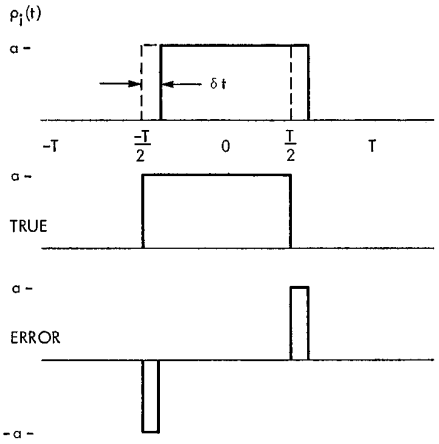

FIG. 9. ZSP–NGP density assignment in time with error term.

For cold plasmas, $\lambda_D = 0$, $N_D = 0$, the physical model has no randomness and, hence, no dispersion. In order to observe plasma oscillations, we gave the electron clouds a small velocity modulation at long wavelength and held the ion clouds fixed, in two dimensions, $H = h$. With the velocity amplitude about one-sixth that needed for the first cloud crossing, we observed almost perfect exchange between potential and kinetic energy for several cycles; at smaller velocity, the exchange was imperfect by a few percent. This defect is partially due to the deviation of the force on individual clouds from the correct force which is dependent on the way the clouds are placed in the grid; Langdon and Wong made this explanation more explicit in one-dimensional theory and experiments [7], with $H = \Delta x$ (large effect) and $H = 10\Delta x$ (vanishingly small grid effect, even out to $kH = 2\pi$).

9. EXPERIENCE WITH CODE

Our experience with the CIC method in two-dimensional plasma problems with code SQuaRPLA has been very good [1]. In initial trial runs we found an appreciable decrease in fluctuations of potential energy as N_D was increased through unity. In subsequent runs, at low density (ω_p^2/ω_c^2 of ions $\lesssim 1$), we found no direct evidence of large angle particle deflections and little or no evidence of particle heating or cooling over hundreds of cyclotron and plasma periods. Perhaps the best measure of confidence has come in the constancy of total energy with no special energy conserving methods used. In spot checks during a plasma build-up run, energy was conserved to within 0.3% for 8000 steps; in another run with 1600 clouds, hot ions and cold electrons in a nonuniform magnetic field, the energy remained constant to within $\pm 0.1\%$ for 5000 steps. Typically, the time step was 1/15 of an electron cyclotron period, 1/40 of an electron plasma period, and about 1/10 of the grid transit time, the mass ratio was $m_i/m_e = 16$. Low-density runs such as these provide little test in trying to distinguish among various methods. These runs were made on the Univac Larc essentially in Fortran II.

In order to compare CIC with ZSP–NGP, computer runs were made on a medium-density warm plasma with identical initial conditions. The plasma had $(\omega_p/\omega_c)_i^2 \cong 14$, was cylindrical in shape bounded by zero potential walls, in a uniform magnetic field, with equal numbers of ions and electrons, mass ratio $m_i/m_e = 16$, with equal kinetic energies for electrons and ions; no particles were lost to the walls. The first pair of runs used 250 electrons with $N_D \cong 3$; the second pair used 5000 electrons (with the charge per cloud decreased in order to keep the plasma frequency constant) with $N_D \cong 60$. The results for the 500 charges are shown in Fig. 12 in the form of energy (total, kinetic, potential) and potential (on two probes in the plasma) versus time. Energy grows in both runs (about 500 times steps) although more slowly for CIC. The fluctuations observed in ZSP–NGP do not appear in CIC and are considered spurious. Results for 10,000 charges are shown in Fig. 13. ZSP–NGP energy increases more slowly (about the same as CIC for 20 times fewer particles). These runs were made on a CDC 6600 using Fortran 400. One CIC time step was about twice as long as that for ZSP–NGP. As most of a step was used in moving the particles, this timing would indicate that ZSP–NGP could use about twice as many particles in the same time. R. Hockney (by letter to us) has noted the same difference in times, also using Fortran, on a gravitational problem (where, incidentally, the equivalent N_D is the total number of particles). As yet, we have little quantitative data on fluctuations relative to theoretical estimates.

10. OTHER APPLICATIONS

Many-body simulation of $1/r$, $1/r^2$ forces with stars uses essentially the same equations given here with a sign change in Poisson's equation. Hence, star calculations of

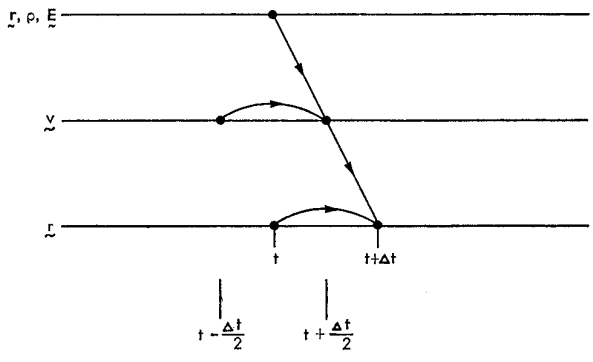

FIG. 10. Equation of motion integration steps.

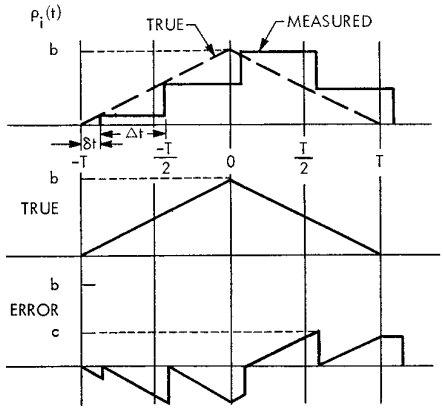

FIG. 11. CIC density assignment in time with error term.

density and force may also use the CIC approach to similar advantage. Each cloud becomes a tenuous collection of stars.

The Vlasov equation using a distribution function, $f(\mathbf{r}, \mathbf{v}, t) = N/d^3x\,d^3v$, could also be solved in a gridded system (in $\mathbf{r}$, $\mathbf{v}$) with clouds of N particles (fixed number) moving about phase space. Use of sharing, CIC, should also help to reduce noise due to computational discreteness.

11. CONCLUSIONS

Contrasts between zero-size-particle, nearest-grid-point and clouds-in-clouds, clouds-in-cells methods of obtaining density and force have been offered. Arguments have been put forth to show that CIC should have substantially less noise or spurious effects than ZSP–NGP, resulting in lower noise for the same N_D if care is used in choosing cloud side H relative to grid side h and λ_D. The transition from ZSP–NGP to CIC coding requires the addition of simple sharing calculations for density and force, adding some time to each step. However, in working with denser and denser plasmas, meaning plasma diameters of more and more λ_D, will put demands on using the least tolerable N_D, to keep the number of particles within computer capacity. Thus CIC should aid in simulating higher density plasmas.

R. L. Morse (Los Alamos Scientific Laboratory) has pointed out that hydrodynamic calculations in their laboratory use their well-known particle-in-cell method (PIC) with ''area weighting,'' analogous to our charge and force sharing, to achieve smoothing. If we claim anything at all, it is that we are among the early users and strong advocates of CIC for simulation of charged particles and plasmas.

We are aware that what is presented here is only a beginning, some initial persuasion and evidence that CIC may be useful. It will be necessary to obtain more rigorous theoretical physical description for clouds interacting with clouds, with and without grids, such as Boltzmann, Vlasov-type equations, collision cross sections and frequencies, dispersion relations, and so on. Such descriptions are being developed [6, 7].

APPENDIX A: POISSON SOLVER

The difference equation used for Poisson's equation is the stencil given by Collatz [8], as follows ($h = \Delta x = \Delta y$):

$$8h^2\nabla^2 u_{0,0} + h^2\nabla^2 u_{1,0} + h^2\nabla^2 u_{0,1} + h^2\nabla^2 u_{-1,0} + h^2\nabla^2 u_{0,-1} + 40u_{0,0} - 8(u_{1,0} + u_{0,1} + \cdot + \cdot) - 2(u_{1,1} + u_{1,-1} + \cdot + \cdot) = 0 + \frac{h^6}{60}\left(3\frac{\partial^6 u}{\partial y^6} + 3\frac{\partial^6 u}{\partial x^6} - 5\frac{\partial^6 u}{\partial x^2\,\partial y^4} - 5\frac{\partial^6 u}{\partial x^4\,\partial y^2}\right) + \cdots .$$

We replaced the $\nabla^2 u$ by the $(-\rho/\varepsilon_0)$ at that grid point. Comparing the error term with the Laplacian terms, for harmonic densities and potentials, shows that this 9-point form produces 1 to 2 orders of magnitude less error at large wavelengths relative to the widely used 5-point form.

The method of solution, for zero potential walls bounding a 48×48 grid, was to Fourier analyze (ρ/ε_0) in x, assume that this could also be done for ϕ, following Hockney (and Buneman [2]), but then to solve the 47 difference equations for each of the 47 harmonics by Gauss elimination; the

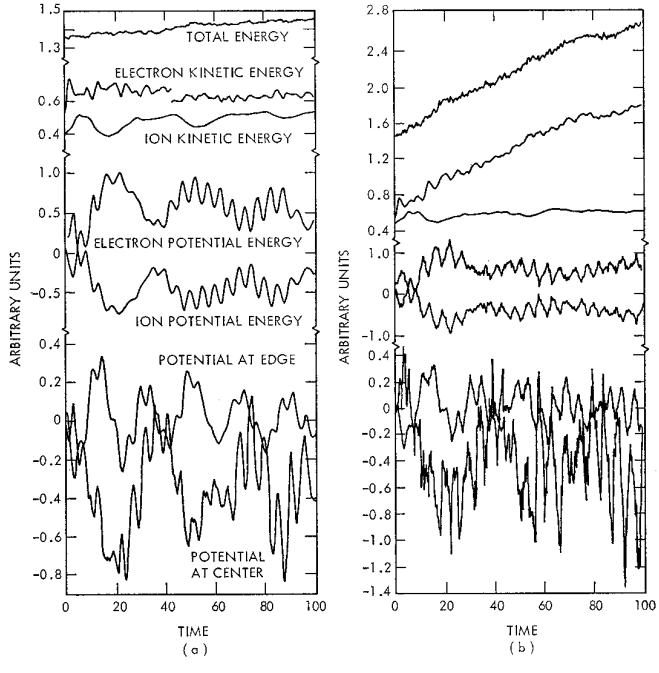

FIG. 12. Comparison runs with 500 particles, (a) for CIC and (b) for ZSP–NGP, in a uniform magnetic field. At $t = 0$, the electron and ion kinetic energies were equal, $m_i/m_e = 16$, $\tau_{pe} \cong 6.7$, $\tau_{pi} \cong 26.9$, $\tau_{ci} = 6.28$, $\tau_{ci} = 100$, $N_D \cong 3$. Run goes to $T \cong 100$. The most prominent frequency appears to be the electron hybrid with calculated period $\tau_H = 4.6$. The ZSP–NGP growth in electron kinetic energy causes the total energy growth—which should not occur physically. There is initial potential energy as the ions and electrons were not overlaid at $t = 0$.

last step is to Fourier synthesize in x to produce $\phi(x, y)$. In the Fourier sine analysis–synthesis, the amplitudes of like-valued sines were gathered together to reduce multiplications; the running times appear comparable with those of more formal fast Fourier transform methods.

For a doubly periodic system with a 32×32 grid, we Fourier analyze the density in both x and y and obtain the Fourier amplitudes of potential directly and then synthesize. We use a FFT routine.

In three dimensions, for zero potential walls bounding a $36 \times 36 \times 36$ grid ($\cong$50,000 points), using a 19-point difference equation [8], the density is Fourier sine analyzed in x and y, then the difference equations are solved for the harmonics of the potential by Gauss elimination, followed by synthesis. Starting with charges on the mesh points, the time for solving for the potential is about 6 seconds, using a Fortran program on the CDC 6600. No attempt has been made to reduce this time, yet it is comparable to that of Hockney's two-dimensional 256×256 ($\cong$65,000 points) highly refined machine code Poisson solver [9].

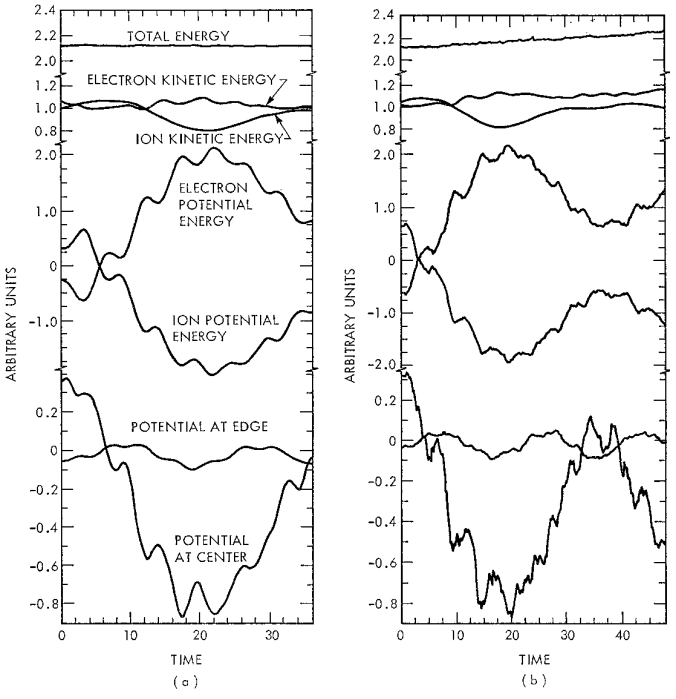

FIG. 13. Same as Fig. 12 but for 10,000 particles and somewhat shorter total time, $N_D \cong 60$. The charge per particle was reduced to maintain the same plasma frequency; the cyclotron frequencies were also the same. The ZSP–NGP spurious effects are much smaller, but total energy still increases.

APPENDIX B: CHARGE SHARING

The charge sharing expression in Section 3 is written out here for the rectangular cloud shown in Fig. 2, $H_x = \Delta x$, $H_y = \Delta y$. The origin for x, y is taken as i, j; x and y must fall within the four grid points named on the figure, accomplished in the code by determining the lower-left-hand grid location (by truncation for $\Delta x = \Delta y = 1$). ρ_c is the charge density of the cloud:

$$\rho(i,j) = \rho_c \frac{(\Delta x - x)(\Delta y - y)}{\Delta x\, \Delta y}$$

$$\rho(i+1,j) = \rho_c \frac{x(\Delta y - y)}{\Delta x\, \Delta y}$$

$$\rho(i+1,j+1) = \rho_c \frac{xy}{\Delta x\, \Delta y}$$

$$\rho(i,j+1) = \rho_c \frac{(\Delta x - x)\, y}{\Delta x\, \Delta y}.$$

ACKNOWLEDGMENTS

We are indebted to many for suggestions, as identified in the text. M. Greenberg, A. B. Langdon, and D. Wong are at the University of California, Berkeley. We have had fruitful exchange with O. Buneman and R. Hockney of Stanford University through quarterly seminars and are especially grateful to Dr. Hockney for his critical review of this paper and constructive criticisms. H. Berk, J. Byers, and C. Leith are at the Lawrence Radiation Laboratory, University of California, Livermore, CA. J. Dawson is at Princeton University, Princeton, NJ. We are also indebted to R. von Holdt (LRL), for mathematical insight in solving Poisson's equation.

REFERENCES

1. C. K. Birdsall and D. Fuss, *Bull. Am. Phys. Soc.* **13,** 283 (1968).
2. R. W. Hockney, Tech. Rep. SUIPR No. 53 (Stanford University, Stanford, CA, May 1966); *Phys. Fluids* **9,** 1862 (1966).
3. C. Barnes and D. A. Dunn, in *Proc. Symposium on Computer Simulation of Plasma and Many-Body Problems, College of William and Mary, Williamsburg, VA, Apr. 19–21, 1967* (NASA SP-153).
4. C. K. Birdsall and W. B. Bridges, *Electron Dynamics of Diode Regions* (Academic Press, New York, 1966, Chap. 6.
5. R. W. Hockney, Tech. Rep. SUIPR No. 202 (Stanford University, Stanford, CA Oct. 1967); also, *Phys. Fluids* **11,** 1381 (1968).
6. J. M. Dawson, C. G. Hsi, and R. Shanny, in *Proc. Conference on Numerical Simulation of Plasma* (Los Alamos Scientific Lab., Los Alamos NM, Sept. 18–20, 1968) (LA-3990).
7. C. K. Birdsall, A. B. Langdon, C. F. McKee, H. Okuda, and D. Wong, in *Proc. Conference on Numerical Simulation of Plasma* (Los Alamos Scientific Lab., Los Alamos, NM, Sept. 18–20, 1968).
8. L. Collatz, *The Numerical Treatment of Differential Equations* (Springer-Verlag, New York, 1966), p. 542 (9-point), p. 546 (19-point).
9. R. Hockney, in *Proc. Conference on Numerical Simulation of Plasma* (Los Alamos Scientific Lab., Los Alamos, NM, Sept. 18–20, 1968).